SAS Journal of Medicine
Abbreviated Key Title: SAS J Med
ISSN 2454-5112
Journal homepage: https://saspublishers.com

OPEN ACCESS

Radiology

Spectrum of CT-Scan Findings in Symptomatic and Asymptomatic Patients of SARS-CoV-2 Disease: An African Series

Nizar El Bouardi[1*], Badreddine Alami[1], Meriam Haloua[1], Youssef Lamrani[1], Meriem Boubbou[1], Mustapha Maaroufi[1]

[1]Radiology Department, Hassan II University hospital, Fez, Morocco

DOI: 10.36347/sasjm.2023.v09i04.002 | **Received:** 15.02.2023 | **Accepted:** 30.03.2023 | **Published:** 02.04.2023

***Corresponding author:** Nizar El Bouardi
Radiology Department, Hassan II University hospital, Fez, Morocco

Abstract **Original Research Article**

In this paper, we studied retrospectively the Chest CT-scan chest of 118 SARS-CoV-2 disease cases confirmed by Polymerase Chain Reaction (PCR). We identified and characterized the most common CT findings, and compared such findings in the asymptomatic patients with those patients that presented with findings in patients with mild form of the disease. Bilateral pulmonary parenchyma ground-glass and consolidative pulmonary opacities, sometimes with a rounded morphology and a peripheral lung distribution were the most common CT findings. These were often associated with reticular and crazy paving pattern. Pleural and pericardial effusions were rare and mainly present in diffuse lung involvement. Most of our patient showed minimal lung involvement. There was no statistical significant difference in CT findings between asymptomatic patients and those with mild symptoms.

Keywords: SARS-CoV-2, pneumonia, computed tomography.

INTRODUCTION

SARS-CoV-2 is an emerging infection caused by a novel coronavirus. Firstly, it appeared in Wuhan city in China in December 2019 when several cases of viral pneumonia were manifested by cough, fever and dyspnea [1]. By January 2020, the disease was still unexplained, and was reported to the world health organization (WHO). Investigations based on broncho-alveolar lavage of samples revealed a virus with a crown morphology characteristic in electron microscopy scanning; due to the presence of viral peplomers spike emanating from the viral envelope [2].

Thus, this virus has been named "2019 novel Coronavirus" which belongs to the family Coronaviridae and the order Nidovarales. The family includes viruses causing SARS (Severe acute respiratory syndrome) and MERS (Middle East respiratory syndrome). The disease has spread all over the world and has been considered by the world health organization (WHO) as a global health emergency on the 30th of January 2020.

In parallel to retro transcriptase-polymerase in chain reaction (RT-PCR), chest imaging showed a highest importance in the diagnosis and management of patients with SARS-CoV-2 infection. Thus, high-resolution computed tomography (HRCT) is used for the early diagnosis. This diagnostic tool allows an objective evaluation of the lung lesions; therefore, enabling understanding of the pathogenesis of the disease [3, 4]. Herein, we report through a retrospective study, the key CT findings in a group of 118 patients infected with the novel Coronavirus in Fez, Morocco. In this first unique African series, we also compared the CT-scan findings in asymptomatic patients and patients with mild clinical disease.

MATERIALS AND METHODS

Patients and Study Design

This retrospective study was achieved in radiology department of the University Hospital of Fez, Morocco. Chest CT-scan data of patients was evaluated. The study was achieved in full agreement with the recommendations of the local ethical committee that comply with the national regulations and the national institute of health (USA) and international standards.

A total of 118 patients were reviewed during the time slot ranging from March 27, 2020 to May 11, 2020. SARS-CoV-2 was confirmed in each patient using a real time RT-PCR samples collected from patient by nasopharyngeal swab by trained medical doctor. All patients underwent a HRCT, acquired in

supine position using Bright Speed 64 slices scanner (General Electric Medical System, Milwaukee, USA). The acquisitions were done using 5 mm slice thicknesses that were reconstructed with 1.25 mm thickness. No iodine contrast agent contrast agent was used. All CT-scan image data were reviewed by two certified radiologists and approved by a highly skilled and trained thoracic radiologist.

CT Review:

The initial CT-scan assessment consisted of recognizing the ground glass opacities, parenchymal consolidation signs, extend of lung involvement, presence of nodules, reverse halo sign, sub-pleural line, pleural and pericardial abnormalities of both thickening and effusion, thoracic lymphadenopathy defined as lymph node with size above 10 mm in short-axis dimension, and presence of an underlying lung diseases such as fibrosis and emphysema. Other findings such as reticulations, interlobular septal thickening, bronchial wall thickening, bronchiectasis and vascular dilatation signs were also recorded. The localization of lesion in various sites was reported.

Degree of lung involvement was classified as bellow:

Minimal involvement is defined as less than 10% of lung involvement (n= 57); moderate involvement for between 10 and 25% (n= 35); extended involvement for between 26 and 50% (n= 20); severe involvement for range between 51 and 75% (n= 4) and critical involvement for values above 75% (n= 2).

Clinical Symptoms:

In our study, four groups of SARS-CoV-2 patients were identified:

- Group 1 (n= 47): included SARS-CoV-2 patients without any clinical symptom but demonstrated lung radiological abnormalities. Most patients of this group were in contact with symptomatic patients that underwent a systematic screening.
- Group 2 (n= 56): included SARS-CoV-2 patients with common symptoms such as fever, cough, and fatigue without any severe breath shortness.
- Group 3 (n=10): included SARS-CoV-2 patients with atypical or uncommon symptoms such as diarrhea, vomiting, ageusia, and anosmia.
- Common symptoms and atypical symptoms reported in groups 2 and 3 were considered as benign clinical form.
- Group 4 (n= 5): included SARS-CoV-2 patients with Severe symptoms including respiratory distress with respiratory rate ≥ 30 times/min in the resting state, and oxygen saturation ≤ 93%, PaO2/FiO2 ≤ 300MMHG. This group included also cases with respiratory failure requiring mechanical ventilation, and other organ failure requiring intensive care monitoring and management.

The statistical analysis was performed using Epi Info (Version 7.1.5, available in March 19, 2015; USA) running in Microsoft Windows environment.

RESULTS

Demographic and Clinical Characteristics (Table 1)

Among 118 patients, 52.54% (n=61) were males and 47.46% (n=56) were females. Their average age was 41.6 years-old.

The asymptomatic patient's rate was 39.30%. The patients with benign symptoms represented 56.41% including 8.50% of patients with atypical symptoms. While only 4.25% patients showed severe signs.

Table 1: Demographic and clinical features of the collected series of SARS-CoV-2 patients

Characteristic	Number	% (CI 95%)
Gender		
Male	62	52.54
Female	56	47.46
Sex ratio	1.1	
Age	3˜81	41.60
Clinical manifestation		
Asymptomatic (group 1)	47	39.31
Benign cases	66	56.41
Common (group 2)	56	47.86
Atypical (group 3)	10	8.50
Digestive symptoms	5	4.25
Sensory symptoms	5	4.25
Severe (group 4)	5	4.25

CT findings (Table 2)

Of the 118 patients, underwent chest CT-scan at admission while 94.06% (n=111) had imaging signs of pneumonia; 87.28% (n=103) of cases showed ground-glass opacities in various forms particularly the nodular form with a rate of 55.30% (n=65); the consolidation was found in 49.15% (n=58) with majority being the nodular form 65.51% (n=38), while

24.57% (n=29) showed reticulations and 10.70% (n=12) contained crazy paving pattern. Besides, 21.18% (n=25) demonstrated sub-pleural lines, and 16.94% (n=20) expressed bronchiectasis. 2.54% (n=3) of patients showed only centro-lobular nodules. The halo sign was present in 38,13% (n=45) accompanying parenchymal consolidations and nodules. Inverted halo sign was present in 4.23% (n=5) of patients and vascular enlargement within the lesions seen in 3.38% (n=4) patients.

Table 2: Summarized computed tomography findings

Characteristic	Number	% (CI 95%)
Distribution		
Unilateral	35	29.66
Bilateral	80	67.79
Subpleural distribution	78	66.10
Lobular distribution	39	33.05
Density		
GGO	103	87.28
Nodular	57	55.33
Diffuse	46	44.64
Condensation	58	49.15
Nodular	38	65.51
Diffuse	20	34.49
Solid nodule	3	2.54
Reticulations	29	24.57
Crazy paving	12	10.70
Subpleural line	25	21.18
Bronchiectasis	20	16.94
Bronchial thickening	2	1.69
Vascular enlargement	4	3.38
Halo sign	45	38,13
inverted Halo sign	5	4.23
Adenopathy	4	3.38
Pleural effusion	3	2.54
Pleural Thickening	6	5.08
Pericardial effusion	1	0.84
Pneumo-mediastinum	1	0.84
Lobes		
Upper lobe	52	44.06
Lower Lobe	86	72.88
Mid lobe	28	23.72
Lung involvement		
<10%	57	48.30
10-25%	35	29.66
25-50%	20	16.94
>50-75%	4	3.38
>75%	2	1.69
Underlying lung disease		
Emphysema	3	2.54
Fibrotic lesions	6	5.08

Lesions with sub-pleural and peripheral distribution were seen in 66.1% (n=78) including bilateral appearance in 67.79% (n=80) of cases and those mostly localized in lower lobes were 72.88% (n=86).

The least frequently revealed lesions were the pleural involvement found in 7.5% (n=9) of patients including pleural thickening in 5% (n=6) of patients, and pleural effusion in 2.5% (n=3) of patients. Only a single patient (0.84%) showed a pericardial effusion. Furthermore, we found an incidental spontaneous pneumomediastinum in another single patient (0.85%). Finally, lymphadenopathy was revealed in 3.38 % (n=4) of patients.

Only 7,62% of patients had a preexisting chronic lung disease consisting in paraseptal pulmonary emphysema in 2,54 % (n=3) and parenchymal fibrosis in 5,08% (n=6).

Regarding the extent of parenchymal lung lesions, 48.30% of patients showed minimal lung involvement with less than 10% of lung involvement,

while 29.66% of patients showed moderate lung involvement ranging between 10 to 25%; 16.94% of patients showed an extended lung involvement ranging from 26 to 50%; 3.38% expressed severe lung involvement ranged between 51 and 75%; and finally 1.69% presented critical lung involvement greater than 75% of the total lung.

Moreover, we analyzed and compared the prevalence of the most frequent lesions including GGO and consolidation in symptomatic and asymptomatic patients. GGO was present in 80.85% (n=38) of asymptomatic patients, and in 83.3% (n=55) of patient with benign clinical forms, while consolidation was found in 55.31% (n=26) of asymptomatic patients, and in 47% (n=31) of patient with a benign clinical form; detailed results are reported in Table 3. On the other hand, 52% of asymptomatic patients showed minimal lung involvement versus 47.5% demonstrated in benign clinical forms, and 30% expressed moderate lung involvement versus 26.2% in benign clinical forms. Thus, we have not found any statistically significant difference in the type and the extent of parenchymal lung lesions in both groups with statistical threshold significance of P-value of 0.05.

Table 3: Prevalence of radiological abnormalities in asymptomatic and symptomatic patients

	Asymptomatic	Benign form
GGO	38 (80.85%)	55 (83.3%)
Consolidation	26 (55.31%)	31 (47%)

DISCUSSION

The Coronaviridae family of viruses includes six known human coronavirus species that are infecting human. Four of these species might cause mild respiratory symptoms similar to the common flu. Epidemics were caused by both beta-coronaviruses species, SARS-CoV in 2002 and MERS-CoV in 2012 infected more than 8000 and 1000 persons respectively [5, 6]. Their mortality rates were not high. The new coronavirus SARS-CoV-2 is the seventh specie of the family with higher infection capability. In May 20th, 2020 more than 5 million cases were recorded over the world, 33% cases were recorded in the USA and 22 % in Europe. Fortunately, it's less lethal than SARS and MERS with more than 319226 deaths (6.5%). In Morocco, 6952 cases were recorded up-to May 18th, 2020, including 2.76% (n=192) of deaths 54% (n=3758) of recovered cases, and 43.18% (n=3002) of active cases. Indeed, it is a major health threat [7].

Most of larger series didn't report statistical significant varying gender predominance. Qifang *et al.*, reported a female predominance (52.17%) [8]; while Yanping *et al.*, reported male predominance 51% [9]. In our study there was a slight male predominance with 52.4% and the sex ratio was 1.1.

Clinically, most patient (80.90%) reported benign symptoms of air-tracts infection including cough (82%), fever (83%), and shortness of breath (31%). Less common symptoms included myalgia (11%), headache (8%) and sore throat (5%). Atypical symptoms remain rare including gastrointestinal symptoms such as diarrhea and vomiting with 2%, and sensory symptoms such as anosmia and ageusia. Large fraction of patients remained asymptomatic varying from 5 to 80% according to the demographic and epidemiologic consideration of each reporting country [10, 11].

Indeed, cough, fever and dyspnea were the most prevailing symptoms in our series. However, 39.30% of our patient's series were asymptomatic while showing frank chest imaging findings, which could be explained by specific epidemiological characteristics of Africa and Middle-East population. Indeed, in May 10, 2020, 6623 cases of SARS- CoV-2 were diagnosed in the university hospital of Fez, Morocco. More than 80% were asymptomatic and/or showed benign clinical signs. Fewer severe forms were documented with average age of 41.6 years and without comorbidities (5), severe forms occurred in elderly patients and/or with comorbidities such as chronic renal failure and diabetes.

The serological diagnostic techniques are the most commonly used to diagnose SARS-CoV-2 infection. Blood cells count changes are most often observed but they are not specific. Leucocytes range can be higher or lower than the normal in 24% and 9% of cases respectively, while being normal in 60-68% of cases. Lymphocytes range showed the most remarkable change, and was below the normal range in 83.30% of cases. Neutrophiles range is increased in 38%. C-reactive protein and D-Dimers are very high in most patients [10].

ELISA kits containing viral nucleoproteins could be used to assess immunoglobulins such as IgM and IgG. Zhang *et al.*, reported infected patients with lower rate of antibodies or below detectable level in the first days of infection. However, there was an increased rate of IgG and IgM antibodies in later days of infection which could be useful for diagnosis purposes [12].

Real-time reverse transcriptase-PCR (RT-PCR) detection is currently the technique of choice for assessing coronavirus because it is specific and a simple quantitative assay. Samples were obtained by nasopharyngeal or oral swab collection. Rectal swab

can also be used in the later days of the diseases in case of negative airway sampling while being symptomatic.

All our patients underwent a nasopharyngeal swab and samples were analyzed using RT-PCR without recording negative cases.

Common CT signs

Abnormal Density: There are 3 types of abnormal density: Ground glasses opacity (GGO), consolidation and GGO with consolidation [13].

GGO is due to a partial alveolar filling by inflammatory cells and plasma. It appears in the early stage of the disease mainly the 4th day. Initially, it expresses a fuzzy margin of inflammatory exudation (figure 1). These exudates subsequently convert to fibro inflammatory proliferates which the GGO margins obvious.

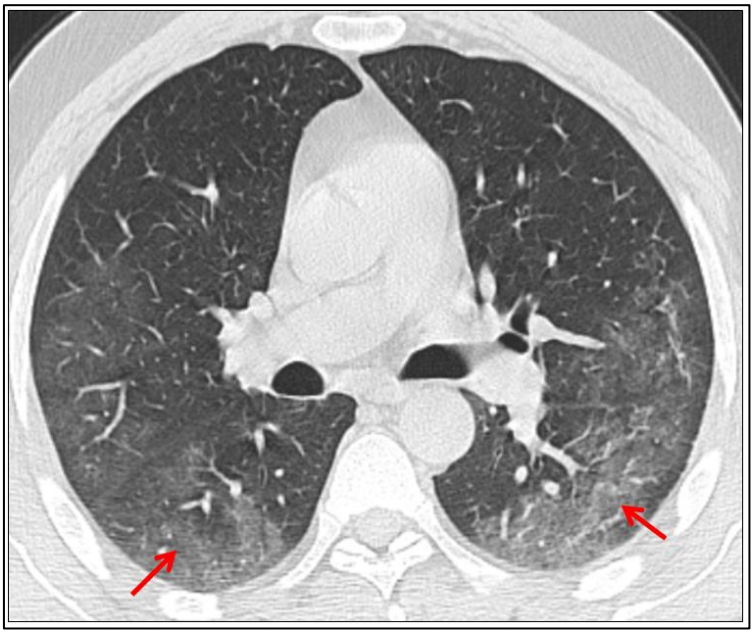

Figure 1: CT scan of a SARS-CoV-2 patient showing a fuzzy diffuse GGO, mainly located peripherally and subpleurally with bilateral lung involvement

GGO opacities will consolidate with frank appearing edge on the 8th day (Figure 2). This consolidation will later have a contracted edge with bronchiectasis and fiber traction on the 14th day.

Both GGO and consolidation share characteristics that will be detailed.

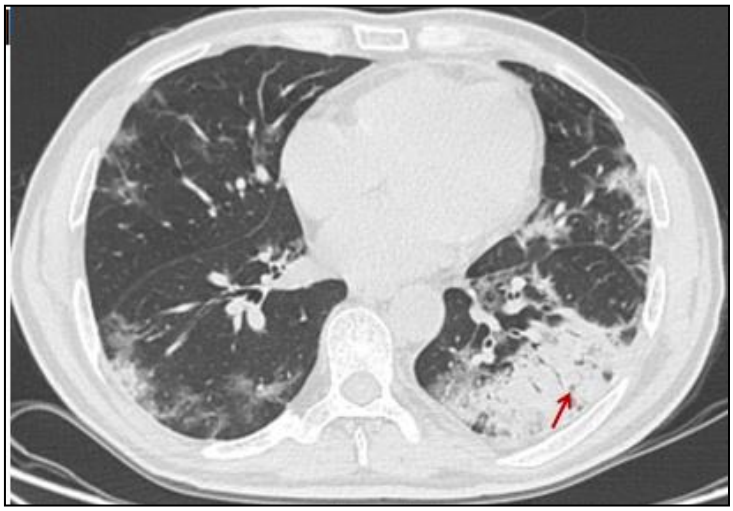

Figure 2: CT scan of a SARS-CoV-2 patient showing mixed GGO and consolidation. Notice a straight edge of consolidation in the left lower lung lobe with air bronchogram (red arrow)

Distribution: The virus mainly invades the bronchioles and originates as bronchiolitis and peripheral inflammation. Then it spreads and further involves the lung tissue in a lobular, subpleural and diffuse patterns as explained below:

- **Lobular Distribution:** The virus causes lobular core inflammation manifesting as globular GGO that quickly diffuse to the adjacent area forming patches of lobular distribution or larger globular GGO. The adjacent lesion will fuse and extend to the surrounding area to involve the lung outer zones or the whole lung.
- **Subpleural Distribution:** Is due to the higher blood and lymph flows in basal and subpleural lung areas leading to more severe inflammation in the lung lobular interstitium. Thus, the distribution is mainly shown in peripheral subpleural region corresponding to the most common distribution patterns.
- **Diffuse Distribution:** Lobular and subpleural distribution can overlap, then progress and merge affecting most areas of the lungs bilaterally causing a diffuse distribution.

Number: The lesions are often multiple and mostly single in very early stage transiting to multiple on follow-up. Multiple lesions might develop and fuse rapidly.

Our results concurred with most of the reviewed series. Jing *et al.*, reported that GGO opacities were present in 53 %, consolidation in 58.40%, and both in 46.20% of patients. They mainly demonstrated a peripheral and subpleural distributions [13]. There was also bilateral lung involvement in 89.30%. The mean lung lobes involved were the lower lobe 74.57%, followed by the upper lobe in 44.06%. The right lower lobe was the most commonly affected. It might be due to the anatomical considerations as the right bronchus is short and vertically oriented hence predisposing the right lower lobe to the causative virus.

Accompanying Signs of Density Abnormalities

Reticular pattern: is defined as thickened pulmonary interstitial tissues such as interlobular septaes and interlobular lines. Reticular pattern are manifesting as smooth thickening of lobular margins in the interlobular septaes in CT images (Figure 3). It might be associated with interstitial lymphocyte infiltration causing interlobular septal thickening [14]. Several studies listed reticular pattern with interlobular septal thickening as the common chest CT-scan expression of SARS-CoV-2 [15-17]. This sign was present in 24.57 % of our cases which is lower than the 35% reported in other series [7].

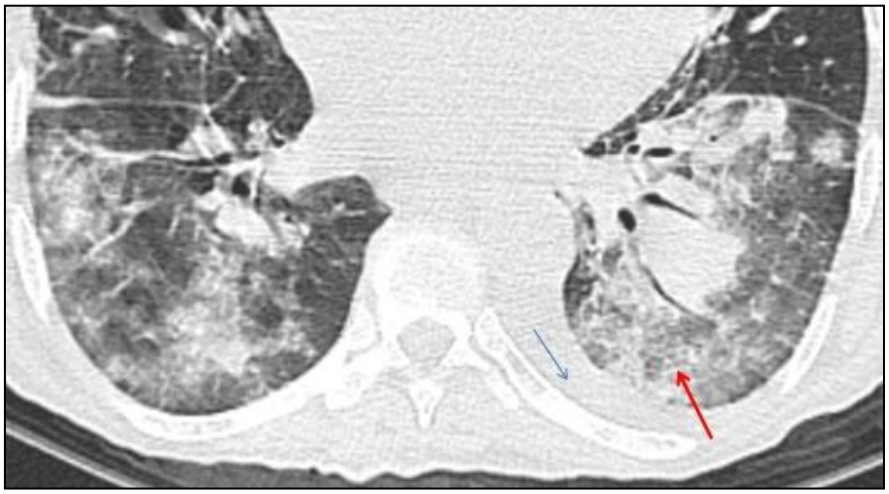

Figure 3: CT scan of a SARS-CoV-2 patient showing patchy GGO and consolidation. There is also a reticular pattern (red arrow). Notice the pleural effusion (blue arrow)

Crazy paving stone sign: The "paving stone sign" is an important sign indicating the virus involvement in the interlobular septum. It is associated with smooth interlobular septal thickening and within GGO opacities. Usually, it precedes the onset of consolidations. This feature is also found in other viral pneumonias such as SARS and MERS and represented 19% to 76.90% [13, 18]. In our series, this occurred in 10% of patients. However, this sign was not specific to other viral pneumonias [19, 20].

Other Signs Apart from Density Abnormalities

Parallel pleura signs: are requiring two conditions, i) the subpleural distribution with the long axis of the lesion that should be parallel to the pleura caused by interlobular and ii) perialveolar lymph drainage directing subpleural and interlobular septum. Actually, the virus invades perilobular and perialveolar intesrtitium. Thus, the lesion will only cling the pleura and spread along the reticular structure of the interlobular septum while diffusing to the periphery. The fusion with subpleural lesions leads to long lesions axes parallel to the pleura. This sign is very

characteristic to SARS-COV-2 and was found in 75.30 % of cases. However, it is not specific since can be found in other interstitial lung diseases and viral pneumonia such as influenza [13].

Air bronchogram: was observed without bronchial obstruction (Figure 2). The virus mainly involves the lung interstitium with little exudation in the alveoli [21]. It was rarely concomitant to bronchial wall thickening. This sign was found in most of our patients with consolidation, it is consistent with the reported literature [18].

Bronchiectasis: This sign occurs as late stage CT-scan finding often accompanied by marginal contraction, suggesting the repair mechanism stage of a lesion caused by fibrous traction. This sign is not specific to SARS-CoV 2, but might be indicative of the disease stage [13]. This sign was present in 40% of cases in our series [13].

Vascular changes: Include vascular enlargement or wall thickening (Figure 4). The inflammation might increase the vascular flow, permeability, telangiectasia and pulmonary artery thickening. Bai *et al.*, found that vascular thickening was significantly associated with SARS-CoV-2 in 59% of patients compared to other viral pneumonia found in 22% ($p<0.001$) [22]. This indicates a vascular enlargement carried specific to COVID-19. In our series, we found a vascular enlargement in 4 patients. Consequently, this sign should be taken into account to distinguish SARS-CoV-2 from other viral pneumonia; this constitutes a principal differential diagnostic feature in CT-scan imaging consideration.

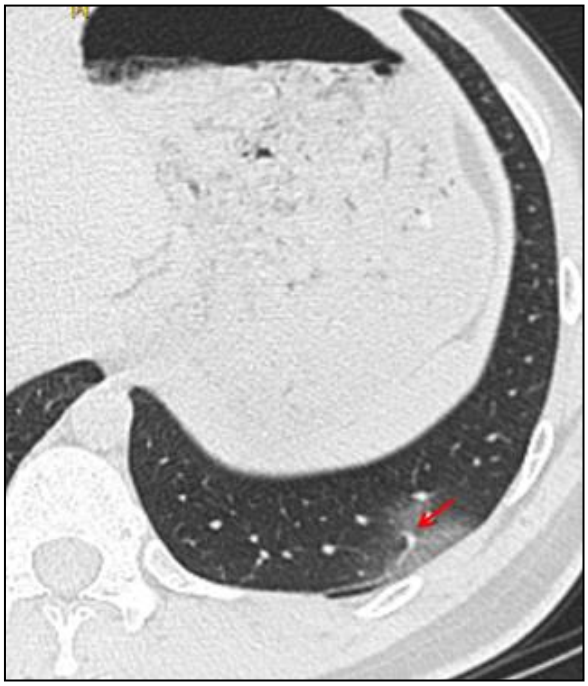

Figure 4: CT scan of a SARS-CoV-2 patient showing a vascular enlargement within GGO

Halo sign and reversed halo sign: Halo sign is defined by ground glass opacity around a nodule or a mass site (Figure 5). It is due to a hemorrhage around the lesion. This sign can be found in SARS-CoV-2. However, it is not specific and can be found in other viral, fungi and vascular lung infections [21].

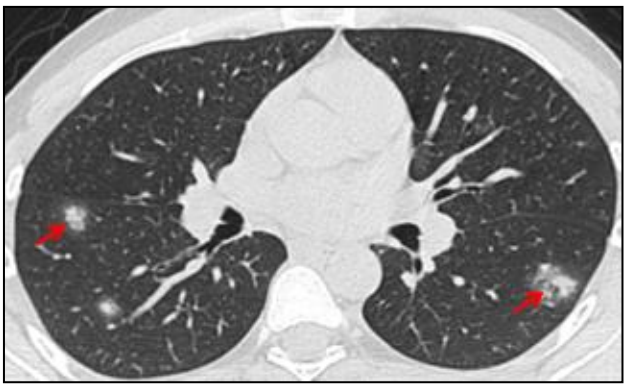

Figure 5: CT scan of a SARS-CoV -2 patient showing nodular consolidation surrounded by a GGO "Halo sign"

Reversed Halo sign is round or half-moon ground glass shape in the center surrounded by high density consolidation (Figure 6). This sign has been reported in SARS-CoV-2 and other lung diseases such as cryptogenic organized pneumonia (COP) [22]. This sign was found in 5 patients in our series. Jing *et al.*, reported this sign in 4.60% (n=6) patients [13].

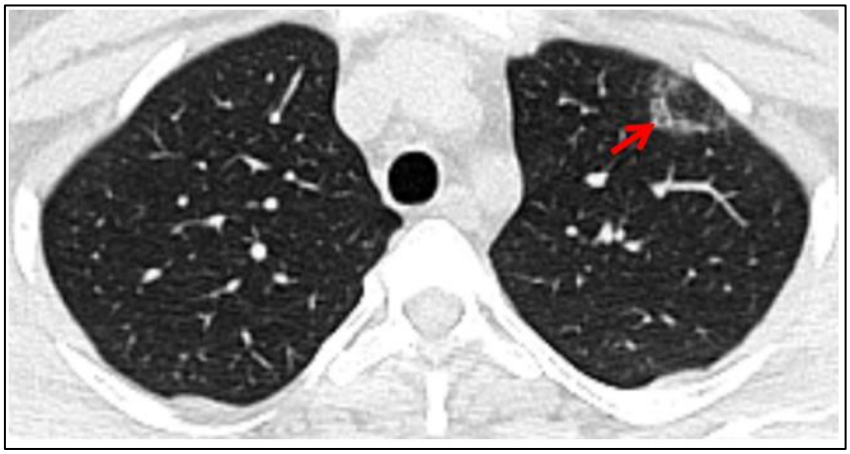

Figure 6: CT scan of a SARS-CoV -2 patient showing a semilunar consolidation surrounding a GGO "Reversed Halo sign"

Nodules: They show round or irregular solid lesions with well or poorly defined edges, they are measuring less than 3 cm in diameter (Figure 5). They are usually subpleural distribution. This sign has been frequently associated with viral pneumonia [17]. Infact, 3 to 13% of COVID-19 patients showed multifocal solid irregular nodules or nodules with visible halo sign [25, 26]. These signs were found in 2.54% (n=3) patients.

Subpleural curvilinear line: was marked by a thin curvilinear opacity of 1 to 3 mm thickness, lying less than 1 cm from and parallel to the pleura (Figure 7). This sign is due to pulmonary edema or fibrosis and seen in 20% of SARS-CoV-2 patients [15, 27], consistent with the 21.40% of our series.

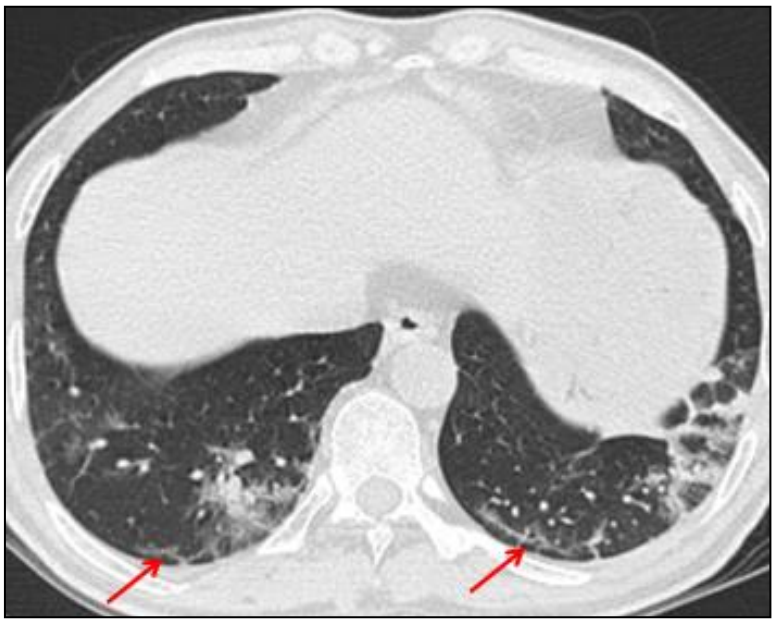

Figure 7: CT scan of a SARS-CoV -2 patient showing a curvilinear subpleural line

Pleural involvement: include pleural effusion and pleural thickening (Figure 8). According to the literature, 32% of patient showed pleural thickening with 5% of pleural effusion [16, 28]. Previous experiences with MERS and influenza, the pleural effusion might suggest a poor prognosis. In our series, 6 patients showed pleural thickening and 3 with pleural effusion. Infact, most of our patients with pleural involvement showed a minimal to moderate lung involvement.

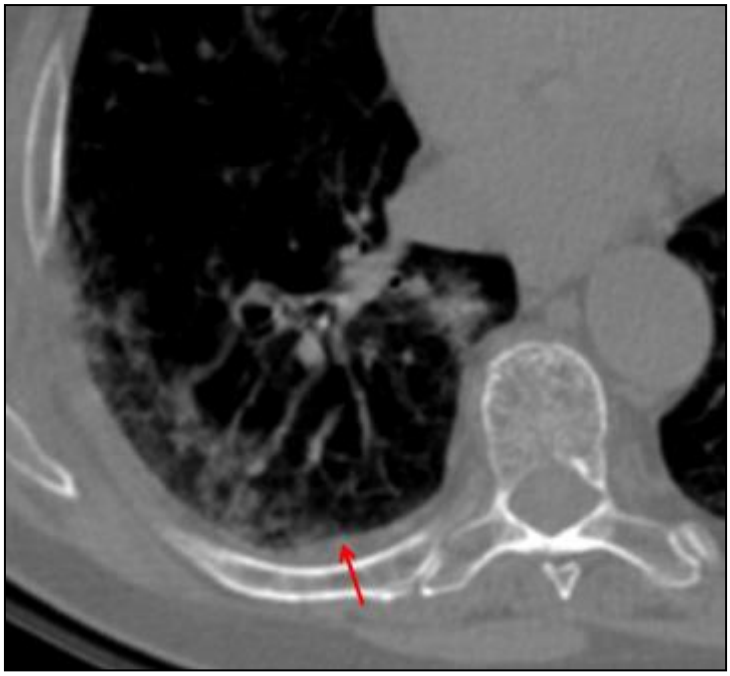

Figure 8: CT scan of a SARS-CoV-2 patient showing a pleural thickening

Pericardial effusion: SARS-CoV-2 patients with a severe inflammation were rare. A higher incidence is shown in severe forms than regular patients [27].

Adenomegaly: The threshold is 1 cm in short axis for mediastinal lymph nodes. They are rare in SARS-CoV-2. They are considered as a significant risk factor for severe pneumonia [27]. However, adenomegaly associated with pleural effusion and tiny lung nodules are suggesting superimposed bacterial infection.

Spontaneous pneumomediastinum: The pathophysiology underlying spontaneous pneumomediastinum is characterized by the presence of a pressure gradient between the alveoli and the lung interstitium resulting in alveolar rupture. The air is accumulated in the interstitium then flows through the venous sheaths to the mediastinum. The pulmonary infection by SRAS-COV-2 causes a breakdown of the alveolar membrane integrity affecting both pneumocytes of type I and II. Consequently, spontaneous pneumomediastinum is more likely to occur when there are extensive pulmonary lesions on CT-scan images expressing the severity of alveolar damage [29].

In our series, the mechanism underlying the pneumomediastinum remains inexplicable. Our patients didn't show predisposing factors of spontaneous pneumomediastinum and didn't present any symptoms. Additionally, there wasn't any extensive parenchymal lesion on CT-scan images (Figure 9). Patients totally recovered without complication during the follow-up.

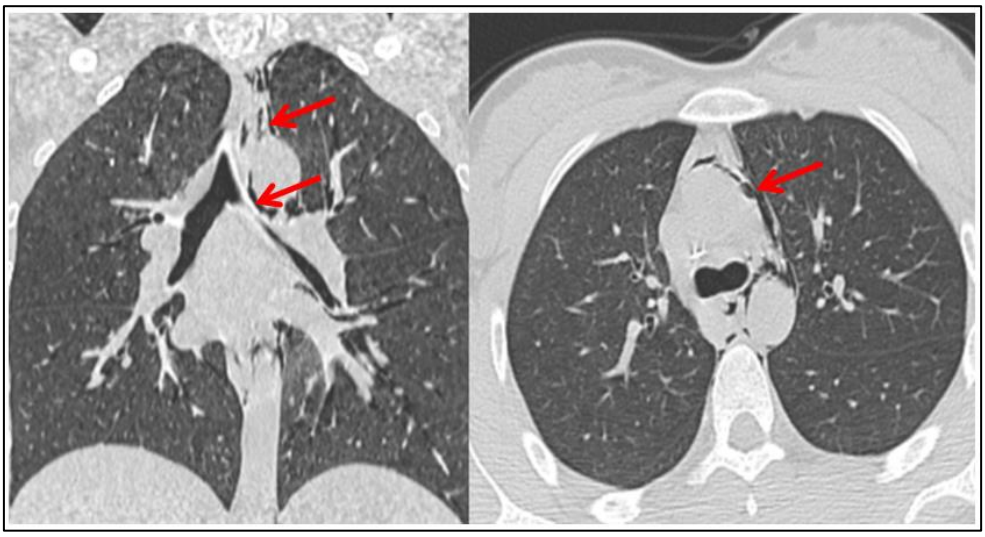

Figure 9: Incidental pneumomediastinum in SARS-CoV-2 patient

Treatment: there was no evidence-based SARS-CoV-2 treatment, but several therapeutic agents were recommended based on randomized controlled trials. However, several therapeutic options suggested include the following:

- Antiviral agents consisting of Lopinavir supplemented by Remdisivir. This combination reduced the mortality from 11% to 2.30% in reported studied patients [30].
- Antimalarial agent comprising either Chloroquine or Hydroxychloroquine showed efficiency in terms of reducing of exacerbation of pneumonia, the duration of symptoms and the delay of viral clearance. Chloroquine or Hydroxychloroquine were recommended as a prophylactic treatment as well as curative treatment of SARS-CoV-2 pneumonia [30].
- Antibiotics supplemented the drug treatments mentioned above and these include; azithromycine, monofloxacin and levofloxacin indicated to prevent bacterial infection.

All patients were hospitalized and underwent a national protocol consisted of 600 mg of hydroxychloroquine administrated for 10 days, this was supplemented by 5 days of azithromycine with 500 mg for the first day and 250 mg for the following days. In case of therapeutic failure or contraindications, patients were treated by antiviral agents consisting of Lopinavir and Ritonavir for additional 10 days. In our series, only five patients were admitted in intensive care unit to support their respiratory distress, all of them had an underlying lung disease. 97.50% (n=115) of patients have recovered, 2.50% (n=3) of patients with poorest prognosis factors passed away following respiratory distress with underlying chronic renal failure, uncontrolled diabetes or aging as co-morbidities.

CONCLUSION

A high rate of patients might demonstrate signs of radiological pneumonia lesions on CT-scan without manifesting any clinical symptoms. Besides, both asymptomatic and symptomatic patients showing benign clinical forms share the same radiological findings with the same lung extent. This study highlighted thoracic CT-scan as a fast, reliable and efficient early diagnosis approach enabling an early primary identification and isolation of SARS-CoV-2 patients, especially asymptomatic cases which exhibit similar features with the symptomatic patients. Bilateral GGO and consolidation were reported as major imaging characteristics in SARS-CoV-2, also common in other viral pneumonia especially SARS and MERS families. The chest CT-scan expressed varying lesional stages and severity depending on the profile and the clinical history of the patient. Thus imaging plays a fundamental role in the rapid identification and early diagnosis of new cases, especially in patients with early negative RT-PCR; hence, enabling better control of the pandemic.

INTEREST CONFLICTS

All authors do not declare any conflict of interests.

REFERENCES

1. Huang, C., Wang, Y., Li, X., Ren, L., Zhao, J., Hu, Y., ... & Cao, B. (2020). Clinical features of patients infected with 2019 novel coronavirus in Wuhan, China. *The lancet*, *395*(10223), 497-506.
2. Chung, M., Bernheim, A., Mei, X., Zhang, N., Huang, M., Zeng, X., ... & Shan, H. (2020). CT imaging features of 2019 novel coronavirus (2019-nCoV). *Radiology*, *295*(1), 202-207.
3. Xie, X., Zhong, Z., Zhao, W., Zheng, C., Wang, F., & Liu, J. (2020). Chest CT for typical coronavirus disease 2019 (COVID-19) pneumonia: relationship to negative RT-PCR testing. *Radiology*, *296*(2), E41-E45.
4. Huang, P., Liu, T., Huang, L., Liu, H., Lei, M., Xu, W., ... & Liu, B. (2020). Use of chest CT in combination with negative RT-PCR assay for the 2019 novel coronavirus but high clinical suspicion. *Radiology*, *295*(1), 22-23.
5. De Groot, R. J., Baker, S. C., Baric, R. S., Brown, C. S., Drosten, C., & Enjuanes, L. (2013). Middle East respiratory syndrome coronavirus (MERS-CoV): announcement of the Coronavirus Study Group. *J Virol*, 87, 7790–92.
6. Zaki, A. M., Van Boheemen, S., Bestebroer, T. M., Osterhaus, A. D., & Fouchier, R. A. (2012). Isolation of a novel coronavirus from a man with pneumonia in Saudi Arabia. *New England Journal of Medicine*, *367*(19), 1814-1820.
7. Shi, H., Han, X., Jiang, N., Cao, Y., Alwalid, O., Gu, J., ... & Zheng, C. (2020). Radiological findings from 81 patients with COVID-19 pneumonia in Wuhan, China: a descriptive study. *The Lancet infectious diseases*, *20*(4), 425-434.
8. Bi, Q., Wu, Y., Mei, S., Ye, C., Zou, X., Zhang, Z., ... & Feng, T. (2020). Epidemiology and transmission of COVID-19 in 391 cases and 1286 of their close contacts in Shenzhen, China: a retrospective cohort study. *The Lancet infectious diseases*, *20*(8), 911-919.
9. The Novel Coronavirus Pneumonia Emergency Response Epidemiology Team. (2020). The Epidemiological Characteristics of an Outbreak of 2019 Novel Coronavirus Diseases (COVID-19) — China. [J]. *China CDC Weekly*, 2(8), 113-122.
10. Ozma, M. A., Maroufi, P., Khodadadi, E., Köse, Ş., Esposito, I., Ganbarov, K., ... & Kafil, H. S. (2020). Clinical manifestation, diagnosis, prevention and control of SARS-CoV-2 (COVID-19) during the outbreak period. *Infez Med*, *28*(2), 153-165.
11. Lovato, A., & de Filippis, C. (2020). Clinical Presentation of COVID-19: A Systematic Review Focusing on Upper Airway Symptoms. *Ear, Nose & Throat Journal*, 99, 569-576.

12. Fox, T., Geppert, J., Dinnes, J., Scandrett, K., Bigio, J., Sulis, G., ... & Cochrane COVID-19 Diagnostic Test Accuracy Group. (2022). Antibody tests for identification of current and past infection with SARS-CoV-2. *Cochrane database of Systematic reviews*, (11).
13. Wu, J., Pan, J., Teng, D., Xu, X., Feng, J., & Chen, Y. C. (2020). Interpretation of CT signs of 2019 novel coronavirus (COVID-19) pneumonia. *European radiology*, *30*, 5455-5462.
14. Hansell, D. M., Bankier, A. A., MacMahon, H., McLoud, T. C., Muller, N. L., & Remy, J. (2008). Fleischner Society: glossary of terms for thoracic imaging. *Radiology*, *246*(3), 697-722.
15. Wu, J., Wu, X., Zeng, W., Guo, D., Fang, Z., Chen, L., ... & Li, C. (2020). Chest CT findings in patients with coronavirus disease 2019 and its relationship with clinical features. *Investigative radiology*, *55*(5), 257-261.
16. Shi, H., Han, X., Jiang, N., Cao, Y., Alwalid, O., Gu, J., ... & Zheng, C. (2020). Radiological findings from 81 patients with COVID-19 pneumonia in Wuhan, China: a descriptive study. *The Lancet infectious diseases*, *20*(4), 425-434.
17. Song, F., Shi, N., Shan, F., Zhang, Z., Shen, J., Lu, H., ... & Shi, Y. (2020). Emerging 2019 novel coronavirus (2019-nCoV) pneumonia. *Radiology*, *295*(1), 210-217.
18. Chung, M., Bernheim, A., Mei, X., Zhang, N., Huang, M., Zeng, X., ... & Shan, H. (2020). CT imaging features of 2019 novel coronavirus (2019-nCoV). *Radiology*, *295*(1), 202-207.
19. Ooi, G. C., Khong, P. L., Müller, N. L., Yiu, W. C., Zhou, L. J., Ho, J. C., ... & Tsang, K. W. (2004). Severe acute respiratory syndrome: temporal lung changes at thin-section CT in 30 patients. *Radiology*, *230*(3), 836-844.
20. Ajlan, A. M., Ahyad, R. A., Jamjoom, L. G., Alharthy, A., & Madani, T. A. (2014). Middle East respiratory syndrome coronavirus (MERS-CoV) infection: chest CT findings. *Ajr Am J Roentgenol*, *203*(4), 782-787.
21. Koo, H. J., Lim, S., Choe, J., Choi, S. H., Sung, H., & Do, K. H. (2018). Radiographic and CT features of viral pneumonia. *Radiographics*, *38*(3), 719-739.
22. Bai, H. X., Hsieh, B., Xiong, Z., Halsey, K., Choi, J. W., Tran, T. M. L., ... & Liao, W. H. (2020). Performance of radiologists in differentiating COVID-19 from non-COVID-19 viral pneumonia at chest CT. *Radiology*, *296*(2), E46-E54.
23. Kim, S. J., Lee, K. S., Ryu, Y. H., Yoon, Y. C., Choe, K. O., Kim, T. S., & Sung, K. J. (2003). Reversed halo sign on high-resolution CT of cryptogenic organizing pneumonia: diagnostic implications. *American Journal of Roentgenology*, *180*(5), 1251-1254.
24. Franquet, T. (2011). Imaging of pulmonary viral pneumonia. *Radiology*, 260, 18–39.
25. Pan, Y., Guan, H., Zhou, S., Wang, Y., Li, Q., Zhu, T., ... & Xia, L. (2020). Initial CT findings and temporal changes in patients with the novel coronavirus pneumonia (2019-nCoV): a study of 63 patients in Wuhan, China. *European radiology*, *30*, 3306-3309.
26. Ai, T., Yang, Z., Hou, H., Zhan, C., Chen, C., Lv, W., ... & Xia, L. (2020). Correlation of chest CT and RT-PCR testing for coronavirus disease 2019 (COVID-19) in China: a report of 1014 cases. *Radiology*, *296*(2), E32-E40.
27. Li, K., Wu, J., Wu, F., Guo, D., Chen, L., Fang, Z., & Li, C. (2020). The clinical and chest CT features associated with severe and critical COVID-19 pneumonia. *Investigative radiology*, 55, 327-331.
28. Bernheim, A., Mei, X., Huang, M., Yang, Y., Fayad, Z. A., Zhang, N., ... & Chung, M. (2020). Chest CT findings in coronavirus disease-19 (COVID-19): relationship to duration of infection. *Radiology*, *295*(3), 685-691.
29. Kolani, S., Houari, N., Haloua, M., Lamrani, Y. A., Boubbou, M., Serraj, M., ... & Alami, B. (2020). Spontaneous pneumomediastinum occurring in the SARS-COV-2 infection. *IDCases*, *21*, e00806.
30. Zhai, P., Ding, Y., Wu, X., Long, J., Zhong, Y., & Li, Y. (2020). The epidemiology, diagnosis and treatment of COVID-19. *International journal of antimicrobial agents*, *55*(5), 105955.